

# Vertex Differentiation Strategy for Tuning the Physical Properties of *closo*-Dodecaborate Weakly Coordinating Anions

*Yessica A. Nelson,<sup>a,b</sup> Ahamed Irshad,<sup>c</sup> Sangmin Kim,<sup>a</sup> Mary A. Waddington,<sup>a</sup> Charlene Z. Salamat,<sup>a</sup> Milan Gembicky,<sup>d</sup> Arnold L. Rheingold,<sup>d</sup> Veronica Carta,<sup>e</sup> Sarah Tolbert,<sup>a,f</sup> Sri R. Narayan,<sup>c</sup> and Alexander M. Spokoyny<sup>a,b</sup>\**

<sup>a</sup> Department of Chemistry and Biochemistry, University of California, Los Angeles, 607 Charles E. Young Drive East, Los Angeles, CA 90095, USA

<sup>b</sup> California NanoSystems Institute (CNSI), University of California, Los Angeles, 570 Westwood Plaza, Los Angeles, CA 90095, USA

<sup>c</sup> Department of Chemistry, University of Southern California, Los Angeles, CA 90089, USA

<sup>d</sup> Department of Chemistry and Biochemistry, University of California, San Diego, La Jolla, California 92093, USA

<sup>e</sup> Department of Chemistry and Biochemistry, University of California, Riverside, Riverside, California 92521, USA

<sup>f</sup> Department of Materials Science and Engineering, University of California, Los Angeles, Los Angeles, CA, 90095, USA

*\*Corresponding Author Information*

E-mail: [spokoyny@chem.ucla.edu](mailto:spokoyny@chem.ucla.edu)

**KEYWORDS** B<sub>12</sub>H<sub>12</sub>, boron cluster, borane, weakly coordinating anions, ionic conductivity

## **ABSTRACT**

We report the synthesis and characterization of various compounds containing 1,7,9-hydroxylated *closo*-dodecahydrododecaborate (B<sub>12</sub>H<sub>9</sub>(OH)<sub>3</sub><sup>2-</sup>) cluster motif. Specifically, we show how the parent compound can be synthesized on the multigram scale and further perhalogenated, leading to a new class of vertex-differentiated weakly coordinating anions (WCAs). We show that a post-modification of the hydroxyl groups by alkylation affords further opportunities for tailoring these anions' stability, steric bulk, and solubility properties. The resulting dodecaborate-based salts were subjected to a full thermal and electrochemical stability evaluation, showing that many of these anions maintain thermal stability up to 500 °C and feature no redox activity below ~1 V vs. Fc/Fc<sup>+</sup>. Mixed hydroxylated/halogenated clusters show enhanced solubility compared to their purely halogenated analogs and retain weakly coordinating properties in the solid-state, as demonstrated by ionic conductivity measurements of their Li<sup>+</sup> salts.

## **INTRODUCTION**

Weakly coordinating anions (WCAs) represent a powerful class of molecules that can enable the formation, isolation, and condensed-phase stabilization of reactive cationic species.<sup>1</sup> For an anion to be considered "weakly coordinating," these species must satisfy several prerequisites, including a low propensity for coordination, chemical stability towards electrophiles, and a large redox stability window. Additionally, some WCAs have low exterior

surface polarizability, showcasing a high degree of charge delocalization, ultimately limiting the presence of accessible basic sites.<sup>2</sup> The latter characteristic is commonly achieved by large spherical and halogenated anions—which can distribute the negative charge over many atoms. Key notable examples of extensively developed classes of WCAs include fluorinated alkoxyaluminates  $[\text{Al}(\text{OR}^{\text{F}})_4]^-$  ( $\text{R}^{\text{F}} = \text{C}(\text{CF}_3)_3$ ) (**Figure 1**, Structure I) and fluorinated (or chlorinated) tetrasubstituted borates  $\text{B}(\text{R}^{\text{F}})_4^-$  ( $\text{R}^{\text{F}} =$  aryl fluorinated organic groups such as  $-\text{C}_6\text{H}_3-3,5-(\text{CF}_3)_2$ , **Figure 1**, Structure II).<sup>2</sup> In these WCA examples, sterically bulky halogenated alkyl or aryl functional groups can tune and enhance the chemical properties and performance of WCAs.<sup>2</sup>

Another class of WCAs that does not necessitate stabilizing halogen-substituted aryl or alkyl groups is based on polyhedral boron clusters.<sup>3</sup> Early pioneering works by Knoth, Reed, and Štíbr developed WCAs using highly symmetrical, three-dimensional polyhedral monocarborane clusters  $[\text{HCB}_{11}\text{H}_{11}]^-$  and  $[\text{HBC}_9\text{H}_9]^-$ .<sup>3</sup> Unfunctionalized monocarborane anions exhibit a large HOMO-LUMO gap with delocalized electron density shared amongst B-B and B-C  $\sigma$  bonds, providing an ideal molecular scaffold for building large, three-dimensional WCA constructs.<sup>3d</sup> Later, both Reed and Štíbr reported halogenated monocarboranes ( $[\text{HCB}_{11}\text{H}_5\text{X}_6]^-$  where X = Cl or Br) (**Figure 1**, Structure III), which show the improved chemical stability of the anion cage by reducing the number of potentially reactive B-H bonds.<sup>3b,g</sup> These early examples showed that boron vertex halogenation could block hydride abstraction by numerous reactive cations such as trityl ( $\text{CPh}_3^+$ ), yielding some of the most chemically robust WCAs known to date.<sup>3</sup> While several subsequent studies have demonstrated the capacity of monocarborane-based WCAs to stabilize various reactive cationic species, their widespread use has been stalled by the lengthy and laborious synthetic processes required to produce parent carborane compounds on a scale.<sup>4</sup>

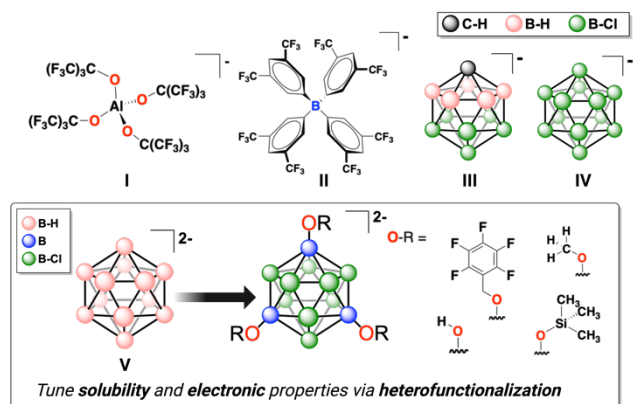


**Figure 1.** Top: Key representative examples of existing WCA. The structures of I, the perfluoroalkoxyaluminate anion  $[\text{Al}[\text{OC}(\text{CF}_3)_3]_4]^-$ , II, the Tetrakis(3,5-bis(trifluoromethyl)phenyl)borate anion  $[\text{BAr}^{\text{F}}_4]^-$  are shown from right to left, III, the partially halogenated monocarborane anion  $[\text{HCB}_{11}\text{H}_5\text{X}_6]^-$ , and IV, the perhalogenated dodecaborate anion  $[\text{B}_{12}\text{X}_{12}]^{2-}$ . Bottom: A new series of mixed halogenated  $[\text{B}_{12}\text{X}_9(\text{OR})_3]^{2-}$  dodecaborates where  $\text{X} = \text{Cl}$  or  $\text{Br}$ , and  $\text{R} = \text{H}$ ,  $\text{CH}_3$ ,  $\text{Si}(\text{CH}_3)_3$ , or  $\text{CH}_2\text{C}_6\text{F}_5$ .

In contrast to monocarboranes, the synthesis of *closo*-dodecaborate  $[\text{B}_{12}\text{H}_{12}]^{2-}$  is straightforward and scalable. Specifically, this cluster can be made on a kilogram scale directly from  $\text{Na}[\text{BH}_4]$  in one step.<sup>5</sup> While dodecaborate anions offer a promising platform for further development, Reed and coworkers have identified the generally lower solubilities of  $[\text{B}_{12}\text{Cl}_{12}]^{2-}$  (**Figure 1**, Structure IV) salts to those of  $[\text{HCB}_{11}\text{H}_{11}]^-$  as a significant limitation in further broad applications.<sup>6</sup>

In this work, we augment the scope of accessible dodecaborate-based WCAs through the development of a mixed hydroxylation/halogenation strategy to generate precisely vertex differentiated cluster species  $[\text{B}_{12}\text{X}_9(\text{OR})_3]^{2-}$  where  $\text{X} = \text{Cl}$ ,  $\text{Br}$ , and  $\text{R} = \text{H}$ ,  $\text{CH}_3$ ,  $\text{Si}(\text{CH}_3)_3$ , or  $\text{CH}_2\text{C}_6\text{F}_5$  (**Figure 1**). Through the developed synthesis, we provide a platform for tuning the solubility of the resulting dodecaborate-based salts, circumventing this previously recognized

limitation. Importantly, we show that a post-modification of the hydroxyl groups by alkoxylation affords further opportunities for tailoring these anions' stability, steric bulk, and solubility properties. The resulting dodecaborate-based salts were subjected to a complete thermal and electrochemical stability evaluation, showing that most of these anions maintain thermal stability up to 500 °C and feature no oxidation below 1 V vs. Fc/Fc<sup>+</sup>. We also provide evidence of enhanced solubility of mixed hydroxylated/halogenated clusters over the corresponding perhalogenated analogues and showcase their retained performance as WCAs through ionic conductivity measurements of the corresponding Li<sup>+</sup> salts in the solid state.

## RESULTS AND DISCUSSION

After the initial discovery of [B<sub>12</sub>X<sub>12</sub>]<sup>2-</sup>, several early pioneers explored various methods to modify [B<sub>12</sub>H<sub>12</sub>]<sup>2-</sup>. Notably, Muetterties reported the hydroxylation of [B<sub>12</sub>H<sub>12</sub>]<sup>2-</sup> by heating N-methyl-2-pyrrolidinone in nitric acid, which can lead to the formation of mono- and disubstituted cluster species.<sup>7</sup> Decades later, a single-step hydroxylation in sulfuric acid was reported by Hawthorne and coworkers.<sup>8</sup> This high-yielding and efficient method offered a higher degree of specificity in hydroxyl addition leading to the isolation of individual [B<sub>12</sub>H<sub>m</sub>(OH)<sub>n</sub>]<sup>2-</sup> clusters where m= 8-11 and n= 1-4. In our early studies delving into the heterofunctionalization of the [B<sub>12</sub>H<sub>12</sub>]<sup>2-</sup> cluster, we employed this method with slight modifications to generate [B<sub>12</sub>H<sub>9</sub>(OH)<sub>3</sub>]<sup>2-</sup> on a multigram scale (**Figure 2** and Figure S1-S2). During the synthesis, the parent B<sub>12</sub>H<sub>12</sub><sup>2-</sup> cluster undergoes a sequential and regioselective acid-catalyzed hydroxylation. Controlling the acid concentration, time, and temperature of this reaction allows one to form the trisubstituted cluster species selectively in a quantitative fashion, as confirmed by *in situ* <sup>11</sup>B NMR spectroscopy. Isolation of the [B<sub>12</sub>H<sub>9</sub>(OH)<sub>3</sub>]<sup>2-</sup> salt is achieved by neutralizing the excess sulfuric acid in the solution and precipitating the dissolved Cs<sub>2</sub>B<sub>12</sub>H<sub>9</sub>(OH)<sub>3</sub> through salt metathesis using

tetrabutylammonium bromide (TBA-Br) giving  $\text{TBA}_2\text{B}_{12}\text{H}_9(\text{OH})_3$ .<sup>8</sup> All spectroscopic characterization of salts containing  $[\text{B}_{12}\text{H}_9(\text{OH})_3]^{2-}$  cluster anions are consistent with the proposed structural formulation (Figure S1-S2).

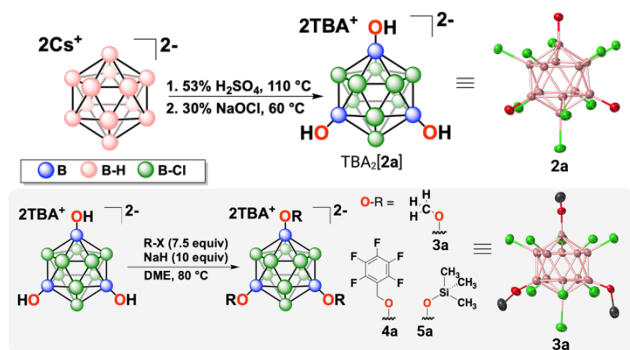


**Figure 2.** Schematic detailing and SCXRD molecular structure (ellipsoids plotted at 50% probability level) of the hydroxylation and subsequent chlorination of  $[\text{B}_{12}\text{H}_{12}]^{2-}$  (top). Continued functionalization of **2a** through alkoxylation **3a**, benzoylation **4a**, and silylation **5a** (bottom).

We hypothesized  $[\text{B}_{12}\text{H}_9(\text{OH})_3]^{2-}$  could be an ideal symmetrical building block amenable to further halogenation and derivatization of the B-OH moieties. Muetterties and coworkers reported the first perchlorinated method of  $\text{Na}_2\text{B}_{12}\text{H}_{12}\cdot 2\text{H}_2\text{O}$  utilizing a silver-lined pressure vessel containing chlorine gas under autogenous pressure.<sup>5b</sup> Later, this method was amended and improved by Uzun *et al.*, who synthesized  $[\text{B}_{12}\text{Cl}_{12}]^{2-}$  on a 10 g scale by bubbling chlorine gas into a solution of  $\text{Na}_2\text{B}_{12}\text{H}_{12}$  for  $\sim 30$  hr.<sup>5a</sup> Subsequently, Ozerov and coworkers have developed a complementary method that does not necessitate the use of chlorine gas and instead utilizes  $\text{SO}_2\text{Cl}_2$  as a chlorinating agent allowing to produce  $[\text{B}_{12}\text{Cl}_{12}]^{2-}$  salts also on a decagram scale.<sup>6b</sup> Duttwyler and coworkers adopted this procedure for the exhaustive perchlorination of a monohydroxylated  $[\text{B}_{12}\text{H}_{11}\text{OH}]^{2-}$  anion producing salts of  $[\text{B}_{12}\text{Cl}_{11}\text{OH}]^{2-}$ .<sup>6c</sup> While the methods above made the desired perchlorinated compounds, we imagined milder chlorinating conditions could be developed to

perchlorinate the B-H vertices of  $\text{Cs}_2\text{B}_{12}\text{H}_9(\text{OH})_3$  without its formal purification and isolation from the aqueous hydroxylation step (*vide supra*).

Sodium hypochlorite is a widely used aqueous chlorinating reagent in organic synthesis.<sup>9</sup> Therefore, we postulated that this reagent could chlorinate the B-H vertices in  $[\text{B}_{12}\text{H}_9(\text{OH})_3]^{2-}$  when introduced to an aqueous solution containing sulfuric acid carried over from the previous synthetic step. To test this hypothesis, we have subjected a solution of  $\text{Cs}_2\text{B}_{12}\text{H}_9(\text{OH})_3$  dissolved in 53% sulfuric acid, with a dropwise addition of excess sodium hypochlorite (6 %) to the reaction mixture. The formation of *in situ*  $\text{Cl}_2$  was visible as a yellow-green gas throughout the addition, consistent with the acid-promoted transformation of the hypochlorite anion.<sup>9</sup> After the addition of sodium hypochlorite is complete, the reaction vessel is stirred for two hours and then heated to 60 °C. Aliquots are then analyzed using *in situ*  $^{11}\text{B}$  NMR spectroscopy to monitor the progress of the reaction. After 24 hours, *in situ*  $^{11}\text{B}$  NMR spectroscopy showed a singlet resonance at -7.2 ppm along with two overlapping resonances, one at -13.5 ppm and another at -15.2 ppm with an integral ratio of 1 to 3, consistent with the expected pattern for the perhalogenated **2a** (Figures 4 and S8-S11) suggesting a complete conversion of the hydroxylated starting material into a new perchlorinated species. The formed product can be precipitated by adding tetrabutylammonium bromide (TBA-Br) directly into the reaction mixture without pH neutralization, followed by filtration of the crude solid product, which is then washed with copious amounts of water to afford pure  $\text{TBA}_2[\mathbf{2a}]$ . All spectroscopic characterization, as well as negative mode ESI(-) mass spectrometry of the isolated product, is consistent with the structural assignment of **2a** (Figures S8-S11). Finally, single crystal X-ray diffraction analysis of  $\text{TBA}_2[\mathbf{2a}]$  crystals grown from a solution of hot ethanol (Figure 2) unequivocally confirmed the proposed structure of  $\text{TBA}_2[\mathbf{2a}]$  and the regioselectivity in hydroxyl group placement along with complete chlorination of the

remaining nine B-H vertices. The bond lengths of the B-O bonds in compound **2a** were determined to be 1.411 Å, 1.403 Å, and 1.435 Å for the 1, 7, and 9 vertices, respectively (**Figure 2** and Table S10). These B-O bond lengths were in close agreement with the B-O bond length of 1.353 Å reported by Duttwyler and coworkers in their study on the monohydroxylated B<sub>12</sub>-based cluster. Importantly, the developed methodology utilizing sodium hypochlorite is not limited to **2a**. For example, upon the reaction of alkali metal salts of unfunctionalized B<sub>12</sub>H<sub>12</sub><sup>2-</sup> with sodium hypochlorite in aqueous media, a complete conversion to the perchlorinated cluster product is observed under similar conditions (Figures S3-S6). This synthesis can be accomplished on at least a decagram scale, making it a convenient and safer alternative to the previously published methods. Additionally, monohydroxylated species (Figure S7) can also be successfully perchlorinated via the same approach, suggesting an overall generality of this method.

With TBA<sub>2</sub>[**2a**] in hand, we decided to investigate whether the B-OH groups on the cluster are amenable to further functionalization. We and others have previously developed and employed multiple procedures for placing functional groups on B-OH moieties in boron clusters that can affect properties such as redox capabilities, hydrophobicity, geometry, and solubility.<sup>10</sup> We initially examined the capability of TBA<sub>2</sub>[**2a**] to undergo alkylation reactions. Reaction optimization utilizing several stoichiometric ratios of TBA[**2a**] and iodomethane in the presence of different bases [*N,N*-diisopropylethylamine (DIPEA), triethylamine (Et<sub>3</sub>N), and NaH] allowed us to develop a high yielding protocol for the methylation of TBA<sub>2</sub>[**2a**]. Under the optimized conditions where 1 equivalent of TBA<sub>2</sub>[**2a**] is stirred with 10 equivalents of NaH and 7.5 equivalents of iodomethane in 1,2-dimethoxyethane (DME) at 80 °C for 0.5 hr, all the starting material is consumed. The desired product TBA<sub>2</sub>[**3a**] is formed as confirmed by negative mode ESI(-) mass spectrometry within 30 min (SI page 11). The major species observed with a mass-to-



charge ratio of 270.4  $m/z$  is consistent with complete methylation of  $\text{TBA}_2[\mathbf{2a}]$  (Figure S12). The reaction is quenched and concentrated under reduced pressure, and the resulting residue is dissolved in dichloromethane, followed by a final purification step using a silica plug. After isolation of  $\text{TBA}_2[\mathbf{3a}]$ , a distinct singlet was observed at 3.5 ppm in the  $^1\text{H}$  NMR spectrum along with four multiplets in an integral ratio of 9:16:16:16:24 (signals corresponding to the  $\text{TBA}^+$  counterion), further suggesting complete methylation of  $\mathbf{2a}$  to  $\mathbf{3a}$  (78 % yield) had occurred (Figure S13). Finally, five resonances were observed in the  $^{13}\text{C}$  spectrum corresponding to four  $\text{TBA}^+$  cation resonances and one resonance at 57.5 ppm corresponding to the methoxy  $\text{B-OCH}_3$  signal (Figure S15). Also,  $\text{TBA}_2[\mathbf{3a}]$  crystals were grown from the slow evaporation of acetone and dichloromethane and analyzed by single crystal X-ray diffraction. The B-O bond lengths in  $\mathbf{3a}$  were determined to have a range of 1.429-1.433 Å. The B-Cl bond lengths in  $\mathbf{3a}$  were found to have a range of 1.779-1.824 Å, which is consistent with the bond lengths observed in  $\mathbf{2a}$  and is also in agreement with previous crystallographic studies of perchlorinated  $\text{B}_{12}$ -based clusters.<sup>6b</sup> Additionally, no significant deviation from the expected structural features of the  $\text{B}_{12}$  cage was observed in the crystal structure of  $\mathbf{3a}$  as determined by single crystal X-ray diffraction analysis (Figure 2 and Table S15).

Having successfully functionalized the three B-OH moieties in the  $\text{B}_{12}^{2-}$  core, we then investigated the feasibility of modifying the system with an electron-withdrawing group such as  $-\text{CH}_2\text{C}_6\text{F}_5$  or with an electron donating group as the  $-\text{OSiMe}_3$ . We followed the general alkylation protocol leading to  $\text{TBA}_2[\mathbf{3a}]$  while using different electrophiles. In both instances, a quantitative conversion of the starting material was observed, resulting in the formation of the corresponding tribenzylated  $\text{TBA}_2\text{B}_{12}\text{Cl}_9(\text{OCH}_2\text{C}_6\text{F}_5)_3$  ( $\mathbf{4a}$ ) and trisilylated  $\text{TBA}_2\text{B}_{12}\text{Cl}_9(\text{OSiMe}_3)_3$  ( $\mathbf{5a}$ ) species with isolated yields of 43% and 73%, respectively (Figure 1 and Figures S16-S24).

To further demonstrate the flexibility of halogen substitution on the trihydroxylated scaffold, a series of brominated derivatives were synthesized. A commonly used brominating method for  $B_{12}H_{12}^{2-}$  is to use excess  $Br_2$  in aqueous methanol.<sup>11</sup> To ensure consistency in our synthetic approach for halogenation, we sought to incorporate  $Br_2$  directly into the acidic solution of  $B_{12}H_9(OH)_3^{2-}$ . Upon testing various reaction conditions, we determined that adding methanol directly to the acidic solution without prior pH neutralization resulted in a successful bromination of the B-H vertices, which can easily be monitored with  $^{11}B$  NMR spectroscopy. After 48 hours, *in situ*  $^{11}B$  NMR spectroscopy showed a singlet resonance at -7.2 ppm along with two overlapping resonances one at -16.8 ppm and one at -19.0 ppm with an integral ratio of 1 to 3, consistent with the expected pattern of a complete conversion of the hydroxylated starting material into a new perbrominated species **2b** (Figures 3 and S27-S30). The **2b** anion was isolated as a TBA<sup>+</sup> salt in a manner similar to **2a** (Figure 3C). The structure of **2b** was confirmed through single crystal X-ray diffraction analysis on crystals grown via vapor-diffusion of ether into acetonitrile. The B-O bond lengths in **2b** were found to be 1.436 Å, 1.424 Å, and 1.413 Å at the 1,7 and 9 vertices, respectively. The average B-O bond length for **2b** was determined to be 1.42(4) Å, which is almost identical with the average B-O bond length for **2a** (1.41(6) Å), despite the presence of bulkier Br groups on the cage (Figure 3C and Table S20). To expand the scope of brominated analogues, we successfully methylated TBA<sub>2</sub>[**2b**], albeit at a slower rate—requiring 18 hours for complete conversion. The major species observed by electrospray ionization was **3b** ( $m/z = 470.71$ ). The slower kinetics associated with the methylation of TBA<sub>2</sub>[**2b**] are likely due to sterically encumbering B-Br bonds surrounding the hydroxyl groups. The same purification steps for TBA<sub>2</sub>[**3a**] were performed to produce TBA<sub>2</sub>[**3b**] (see SI S24).

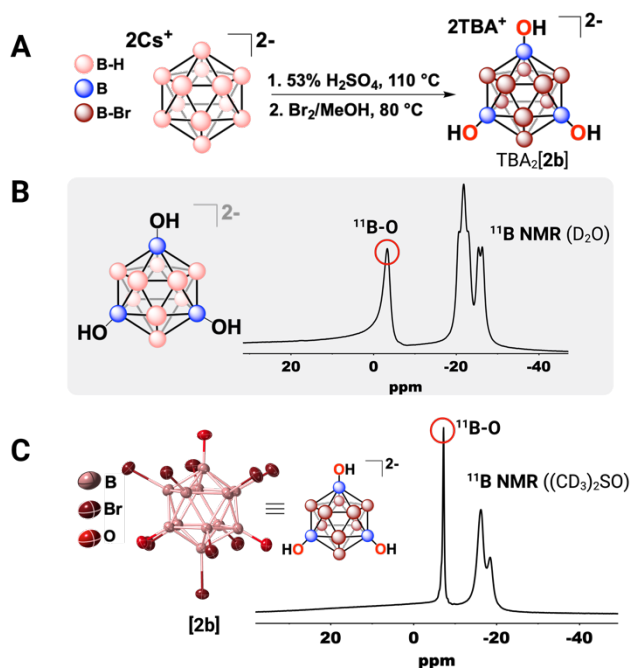


**Figure 3.** A. Synthetic scheme to produce the brominated derivative **2b** achieved through general hydroxylation procedure and single-step bromination using  $\text{Br}_2$  in methanol. B.  $^{11}\text{B}$  NMR spectrum of isolated  $[\text{B}_{12}\text{H}_9(\text{OH})_3]^{2-}$  species in  $\text{D}_2\text{O}$ . C. X-ray single crystal diffraction structure outlining the 1,7,9 hydroxylated vertices of the  $\text{TBA}_2[\mathbf{2b}]$  compound and the accompanying  $^{11}\text{B}$  NMR in  $(\text{CD}_3)_2\text{SO}$  of  $\text{TBA}_2[\mathbf{2b}]$ .

Having a small library of  $\text{TBA}^+$  salts containing various heterofunctionalized perhalogenated  $\text{B}_{12}^{2-}$ -based anions, we decided to explore the feasibility of exchanging tetraalkylammonium cation into an alkali metal cation. Specifically, we decided to use  $\text{Li}^+$ , considering previously reported Li-based boron cluster systems, which exhibited significant ion mobility due to the weakly coordinating nature of the boron cluster building blocks comprising these materials.<sup>12</sup> We employed a resin-based cation exchange method adapted from a report by Strauss and coworkers to convert the organic cation into the  $\text{Li}^+$  cation.<sup>13</sup> The process involved dissolving  $\text{TBA}_2[\mathbf{2a}]$  in a 1:1 solution of acetonitrile and methanol, passing the solution through a column packed with Amberlyst-15 proton resin exchange beads saturated in the same solvent, and

collecting the eluent as a hydronium salt solution (see Figures S35-S36 for a representative characterization of  $(\text{H}_3\text{O}^+)_2[\mathbf{2a}] \cdot n\text{H}_2\text{O}$ ).<sup>13</sup> The eluted solvent mixture was removed under reduced pressure, producing an oily residue. The residue was then dissolved in water, and the pH was adjusted to neutral using a 0.05 mM aqueous solution of LiOH. The final product  $\text{Li}_2[\mathbf{2a}]$  was obtained by drying the mixture *in vacuo*, resulting in a white solid powder product. Analysis of  $\text{Li}_2[\mathbf{2a}]$  through  $^1\text{H}$  NMR,  $^7\text{Li}$  NMR,  $^{13}\text{C}$  NMR, and  $^{11}\text{B}$  NMR spectroscopy provided evidence for the successful isolation of the lithium salt (**Figures 4** and S38). This method can also be successfully applied to the TBA<sup>+</sup> salts of **1a**, **1b**, **2b**, **3a**, and **3b**. Upon thermal activation (see the section below for further discussion), the  $^1\text{H}$  NMR spectroscopy of **1a**, **1b**, **2a**, **2b**, **3a**, and **3b** cation-exchanged salts revealed a singlet resonance at 4.8 ppm, corresponding to the residual solvent peak of  $\text{D}_2\text{O}$ , confirming the removal of the organic cation as supported by the sample data presented in **Figure 4B** for **2a**. The analysis of these lithium salts through  $^7\text{Li}$  NMR,  $^{13}\text{C}$  NMR, and  $^{11}\text{B}$  NMR spectroscopy provided additional evidence for the isolation of the lithium salts, as depicted in Figures S37-S42. Specifically, the  $^1\text{H}$  NMR spectrum for  $\text{Li}_2[\mathbf{3a}]$  contained only a singlet resonance at 3.7 ppm, ascribed to the methoxy B-OCH<sub>3</sub> signal (Figure S39). As with  $\text{Li}_2[\mathbf{3a}]$ , the  $^1\text{H}$  NMR and  $^{13}\text{C}$  NMR spectra of  $\text{Li}_2[\mathbf{3b}]$  contained single resonances corresponding to methoxy at 3.7 ppm and 54.8 ppm, respectively (Figure S42). This data confirms the isolation of Li<sup>+</sup> salts of all products with an average yield of 86-90%.

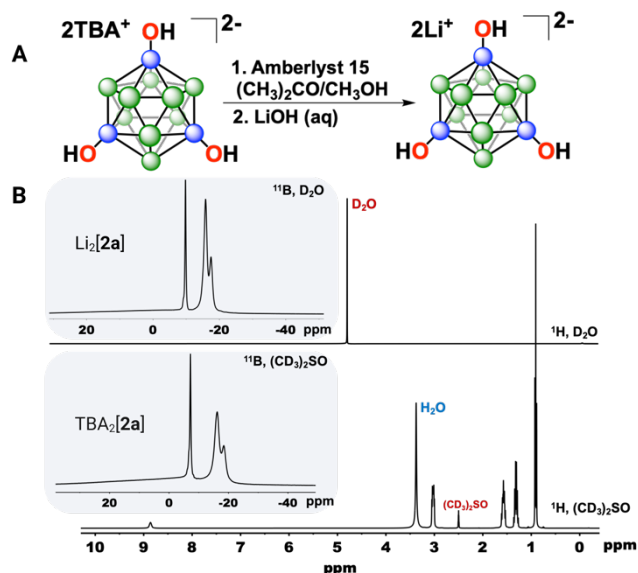


**Figure 4.** A. Scheme for cation exchange. B. Comparison of  $^{11}\text{B}$  and  $^1\text{H}$  NMR spectra of  $\text{Li}_2[\mathbf{2a}]$  and  $\text{TBA}_2[\mathbf{2a}]$ , respectively.

In our cation-exchange study, we observed that the solubility of the  $\text{Li}_2[\mathbf{1a}]$ ,  $\text{Li}_2[\mathbf{2a}]$ , and  $\text{Li}_2[\mathbf{3a}]$  salts were significantly enhanced in water. This observation prompted us to investigate the influence of mixed halogenation and hydroxylation on solubility enhancement in other solvents of varying polarities, including methanol, acetonitrile, dichloromethane, and tetrahydrofuran. Through a series of experiments, we observed an enhancement in solubility of the  $\text{Li}_2[\mathbf{1a}]$ ,  $\text{Li}_2[\mathbf{2a}]$ , and  $\text{Li}_2[\mathbf{3a}]$  where the results are summarized in **Figure 5**.

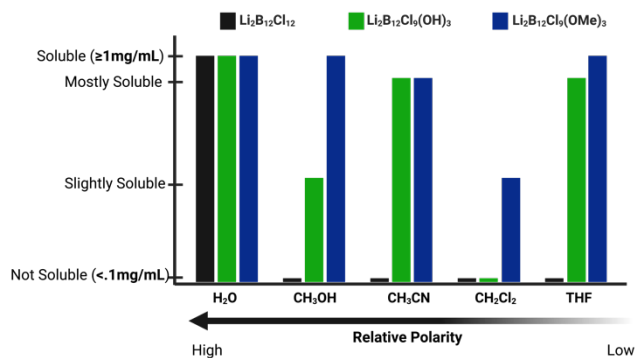


**Figure 5.** Bar chart summarizing solubility studies, across various polarities of common solvents, of  $\text{Li}_2\text{B}_{12}\text{Cl}_{12}$  (**1a**) (black),  $\text{Li}_2\text{B}_{12}\text{Cl}_9(\text{OH})_3$  (**2a**) (green), and  $\text{Li}_2\text{B}_{12}\text{Cl}_9(\text{OMe})_3$  (**3a**) (blue).

$\text{Li}_2[\mathbf{1a}]$  was largely insoluble in all the solvents tested, except for water, which is consistent with previous reports.<sup>6c</sup> The solubility of  $\text{Li}_2[\mathbf{2a}]$ , a lithium cluster containing hydroxyl groups, was found to be improved in all solvents except for  $\text{CH}_2\text{Cl}_2$ . Moreover,  $\text{Li}_2[\mathbf{3a}]$ , a lithium cluster containing methyl groups, demonstrated increased solubility in all solvents, including  $\text{CH}_2\text{Cl}_2$ . Parenthetically,  $\text{Li}_2[\mathbf{3a}]$  exhibits significant hygroscopic characteristics in that a thermally activated 3.50 mg sample absorbs 0.50 mg of water in ~27% humidity air within 1 minute, and after 2 hours a total of 0.72 mg of water is absorbed by  $\text{Li}_2[\mathbf{3a}]$ . Overall, our findings suggest that mixed vertex modification can be an effective strategy for enhancing the solubility of perhalogenated  $\text{B}_{12}$ -based compounds in various solvents.

Previously developed  $\text{Li}^+$ -based boron clusters containing superionic conductors showed the most promising conductivities at elevated temperatures.<sup>12a, c</sup> We, therefore, set out to study the effect of mixed hydroxylation/halogenation on the thermal and oxidation stability of this new library of *closo*-dodecaborates as lithium salts using thermogravimetric analysis and cyclic voltammetry. As a comparative study to the perchlorinated  $\mathbf{1a}$  cluster, we subjected the  $\text{Li}_2[\mathbf{2a}]$  salt to a thermogravimetric analysis to temperatures from 60 °C to 1000 °C under a flow of  $\text{N}_2$  at a rate of 10 °C/min. The results summarized in **Figure 6A**, demonstrate a 14% dehydration, corresponding to only two water molecules per lithium, possibly due to the coordination of the anion's hydroxyl groups to the alkali metal. At the elevated temperatures ranging from 200 °C to 500 °C, mass loss of the sample is negligible. However, after 500 °C, a rapid loss of 20% in the sample weight is observed, suggesting mixed halogenation only minimally reduces the thermal stability of the anion scaffold when compared to its perhalogenated analogue ( $\text{Li}_2[\mathbf{1a}]$ ). After initial dehydration corresponding to the loss of three water molecules per lithium, the heating of  $\text{Li}_2[\mathbf{3a}]$

resulted in the most significant weight change profile as ~10% loss is observed at just 250 °C. Continued mass loss is observed as heating extends to 1000 °C resulting in an overall 80% reduction in sample weight. The significant impact of methylation upon anion stability was initially thought to be a possible result of thermally induced lithium chloride-catalyzed demethylation, which Bei and coworkers previously observed under microwave conditions for aryl methyl ethers.<sup>14</sup> Further studies are needed to substantiate this hypothesis.

Thermogravimetric analysis was also performed on the library of brominated Li<sup>+</sup> salts. Samples of Li<sub>2</sub>[**1b**], Li<sub>2</sub>[**2b**], and Li<sub>2</sub>[**3b**] were dehydrated by 8%, 15%, and 11%, corresponding to the coordination of three, four, and three water molecules to lithium, respectively (**Figure 6B**). Heating Li<sub>2</sub>[**1b**] beyond 200 °C resulted in no significant mass change until 800 °C, where 80% of the sample weight was lost, which is in agreement with previously reported results on the perbrominated cluster.<sup>11</sup> Heating Li<sub>2</sub>[**2b**] beyond 200 °C resulted in little weight (%) change until 500 °C, after which continuous mass loss was observed—indicating Li<sub>2</sub>B<sub>12</sub>X<sub>9</sub>(OH)<sub>3</sub> salts have similar thermal stability to their chlorinated congeners. Finally, continued weight (%) loss was observed in the thermogravimetric curve of Li<sub>2</sub>[**3b**] across the thermal ramp from 60 °C to 1000 °C suggesting thermally induced reactivity was likely occurring in heated samples of both Li<sub>2</sub>[**3a**] and Li<sub>2</sub>[**3b**]. Despite the decrease in thermal stability observed with the trimethylated compounds, the trihydroxylated derivatives exhibit overall similar thermal stability as the perhalogenated derivatives, as evidenced by the retention of structural integrity up to 500 °C for Li<sub>2</sub>[**2a**] and Li<sub>2</sub>[**2b**] salts. This outcome suggests that the type of halogen (X= Cl or Br) did not substantially impact thermal stability, and halogen modulation could be used to modify the resulting salt's steric and solubility properties.

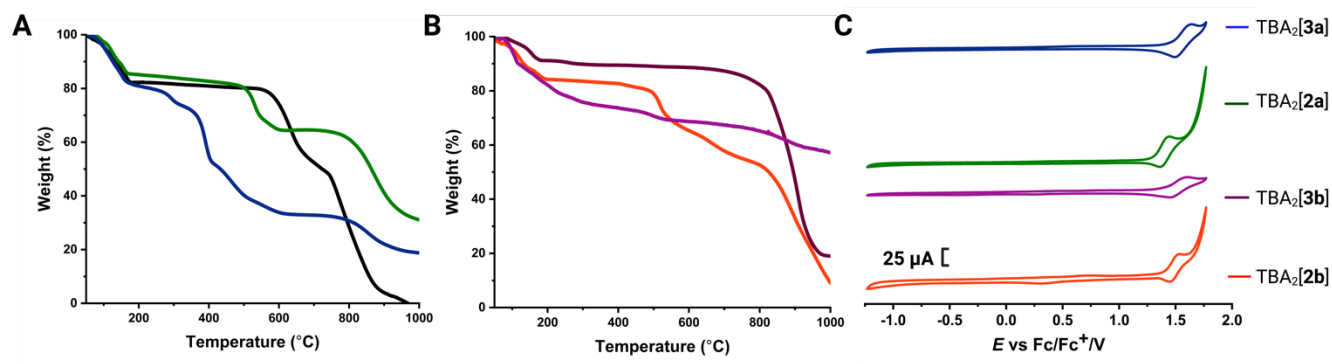


**Figure 6.** A. Thermogravimetric analysis (TGA) of  $\text{Li}_2[1]$  (black),  $\text{Li}_2[2a]$  (green), and  $\text{Li}_2[3a]$  (blue) B. Thermogravimetric analysis (TGA) of  $\text{Li}_2[1b]$  (brown),  $\text{Li}_2[2b]$  (orange), and  $\text{Li}_2[3b]$  (purple). Samples were heated at a rate of  $10\text{ }^\circ\text{C}/\text{min}$  under a constant flow of argon ( $200\text{ mL}/\text{min}$ ). C. Cyclic Voltammograms (CVs) of **2a** (green), **2b** (orange), **3a** (blue), and **3b** (purple) at a scan rate of  $100\text{ mV}/\text{s}$  in  $1\text{M LiTFSI}$  in EC: DMC (50:50) with a Li as a counter and reference and glassy carbon as a working electrode at room temperature externally referenced to  $\text{Fc}/\text{Fc}^+$ .

In continuation of our investigation into the stability of these new compounds, we next evaluated the electrochemical properties of  $\text{TBA}_2[2a]$ ,  $\text{TBA}_2[2b]$ ,  $\text{TBA}_2[3a]$ , and  $\text{TBA}_2[3b]$  by cyclic voltammetry (CV). The voltammogram of  $\text{TBA}_2[2a]$  (**Figure 6C**) displayed one reversible, one-electron redox event assigned to the  $[2a]^{2-/1-}$  couple at  $+1.41\text{ V}$  vs.  $\text{Fc}/\text{Fc}^+$ . Similarly, voltammograms of  $\text{TBA}_2[2b]$ ,  $\text{TBA}_2[3a]$ , and  $\text{TBA}_2[3b]$  showed one reversible, one electron redox event assigned to the  $2-/1-$  at  $+1.18\text{ V}$ ,  $+1.10\text{V}$ ,  $+1.03\text{ V}$  vs.  $\text{Fc}/\text{Fc}^+$  respectively (**Figure 6C**, Figures S43-S48). To corroborate the electrochemical data, we calculated the difference between the highest occupied molecular orbital (HOMO) and lowest unoccupied molecular orbital (LUMO) of each cluster optimized based on the crystallographic structures using the GGA-PBE-D3(BJ) functional and a DZP basis set (**Figure 7** and see SI S35-41). Our calculations reveal that **1a** exhibits the highest HOMO-LUMO energy gap of  $4.25\text{ eV}$ , followed by **2a** with a gap of  $3.72\text{ eV}$ .



A trend in decreasing the HOMO-LUMO gap is observed in the order of **1a** > **2a** > **1b** > **2b** > **3a** > **3b**. Notably, the smallest HOMO-LUMO gap (**3b**) does not fall below 3.04 eV, indicating a high level of electrochemical stability for the entire library of clusters.<sup>10b,15</sup> Moreover, our calculations are consistent with our experimental electrochemical observations, demonstrating the retained oxidation stability at high potentials of these clusters.

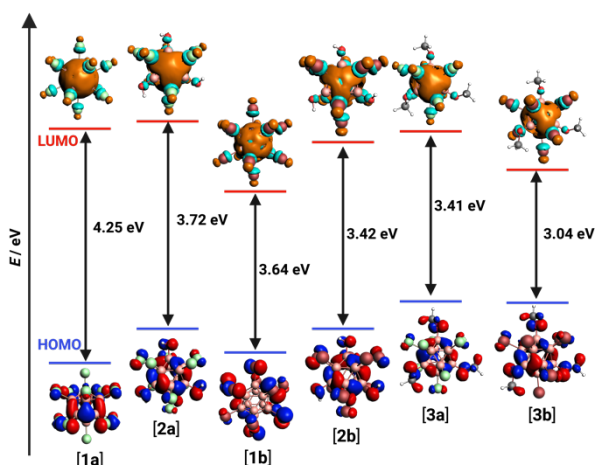


**Figure 7.** Kohn-Sham representations of the HOMO (red, blue) and LUMO (orange, cyan) energies of **1a**, **1b**, **2a**, **2b**, **3a**, and **3b**, calculated from the corresponding optimized crystallographic structures using GGA: PBE-D3(BJ) functional DZP basis set.

Ionic conductivity in B<sub>12</sub>-based boron clusters is generally achieved by thermally induced disorder in the structure, where the large, weakly coordinating anions rotate, creating a dynamic environment for the easy movement of cations.<sup>12</sup> To compare our library of mixed halogenation/hydroxylation B<sub>12</sub>-based Li<sup>+</sup> salts to established cluster-based WCAs, we set out to determine the ionic conductivity of the different clusters by electrochemical impedance spectroscopy (EIS).<sup>12</sup> By analyzing the chemical nature of the anion on the conduction mechanism, we determined that the total ionic conductivity is mediated only by Li<sup>+</sup> (cation) conduction—with

no contribution from the core of the cage or any other functional groups.  $\text{Li}_2\text{B}_{12}(\text{OH})_{12}$  was used as a control, with a measured conductivity of  $8.9 \times 10^{-4} \text{ S cm}^{-1}$  at  $300 \text{ }^\circ\text{C}$  (see Figure 8 and SI S41-S42), which is in agreement with a recently reported study by Jørgensen and coworkers.<sup>12b</sup>  $\text{Li}_2[\mathbf{1a}]$  has a conductivity of  $4.0 \times 10^{-4} \text{ S cm}^{-1}$  at  $300 \text{ }^\circ\text{C}$ , and  $\text{Li}_2[\mathbf{2a}]$  has a conductivity of  $7.6 \times 10^{-4} \text{ S cm}^{-1}$  at  $300 \text{ }^\circ\text{C}$ . The high-temperature ionic conductivity of  $\text{Li}_2[\mathbf{2a}]$  is similar to that of  $\text{Li}_2\text{B}_{12}(\text{OH})_{12}$ .

In the  $\text{Li}_2\text{B}_{12}\text{Cl}_{12}$  and  $\text{Li}_2\text{B}_{12}(\text{OH})_{12}$  perfunctionalized analogues, the inert sphere undergoes a thermal polymorphic transition which facilitates anion reorientations, contributing to the cation diffusion and overall high ionic conductivity.<sup>12a,b,16</sup> Additionally, the low activation barriers in the energy interactions between cations and anions in a solid-state environment further facilitate ion diffusion and conductivity.<sup>12,16</sup> This high ionic conductivity confirms the retention of WCA character in the solid state for these  $\text{Li}^+$  salts.<sup>12,16</sup>

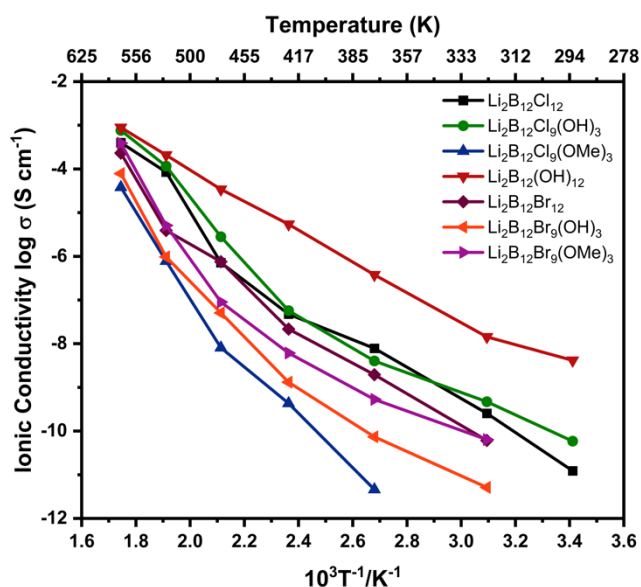


**Figure 8.** Arrhenius plots of the lithium-ion conductivities for **1a**, **1b**, **2a**, **2b**, **3a**, **3b**, and **4**.

The high ionic conductivity of  $\text{Li}_2[\mathbf{2a}]$  at elevated temperatures suggests it is likely to have similar properties to  $\text{Li}_2\text{B}_{12}\text{Cl}_{12}$  and  $\text{Li}_2\text{B}_{12}(\text{OH})_{12}$ . These results suggest that the polyfunctionalization of

perhalogenated B<sub>12</sub>-based clusters with hydroxyl groups can lead to a class of weakly coordinating anions with tunable ion conductivity properties.

## CONCLUSION

With this work, we have introduced a series of heterofunctionalized perhalogenated closedodecaborate clusters containing three hydroxyl groups which can be used as convenient handles for post-synthetic modification [B<sub>12</sub>X<sub>9</sub>(OR)<sub>3</sub>]<sup>2-</sup> (X= Br, Cl, and R= H, CH<sub>3</sub>, Si(CH<sub>3</sub>)<sub>3</sub>, or C<sub>6</sub>H<sub>5</sub>CH<sub>2</sub>). Specifically, we show how these new anionic clusters can be made via straightforward and operationally simple protocols on a multigram scale. The presence of the B-OR sites in these species provides an ability to tune solubility, redox, and thermal stability properties in these clusters. Furthermore, ionic conductivity measurements on the Li<sup>+</sup> salts of these anions suggest that the introduction of B-OR moieties retain the weakly coordinating properties of these clusters. Considering the exceptionally high thermal stability (500 °C) of some of the newly synthesized materials, we believe that these molecules have the potential for further exploration in the areas of synthesis and material science.

## ASSOCIATED CONTENT

### Supporting Information.

The following files are available free of charge.

Detailed experimental procedures, characterization data, crystallographic, computational data, and spectroscopy (PDF)

X-ray crystallographic data for **2a** (CIF)

X-ray crystallographic data for **2b** (CIF)

X-ray crystallographic data for **3a** (CIF)

Accession Codes: CCDC 2251542, 2251541, 2251538 contain the supplementary crystallographic data for this paper. These data can be obtained free of charge via [www.ccdc.cam.ac.uk/data\\_request/cif](http://www.ccdc.cam.ac.uk/data_request/cif), or by emailing [data\\_request@ccdc.cam.ac.uk](mailto:data_request@ccdc.cam.ac.uk), or by contacting The Cambridge Crystallographic Data Centre, 12 Union Road, Cambridge CB2 1EZ, UK; fax: +44 1223 336033

## **AUTHOR INFORMATION**

### **Corresponding Author**

**\*Alexander M. Spokoyny** - *Department of Chemistry and Biochemistry, University of California, Los Angeles, Los Angeles, California 90095, United States; California NanoSystems Institute, University of California, Los Angeles, Los Angeles, California 90095, United States; <https://orcid.org/0000-0002-5683-6240>; Email: [spokoyny@chem.ucla.edu](mailto:spokoyny@chem.ucla.edu)*

**Yessica A. Nelson** - *Department of Chemistry and Biochemistry, University of California, Los Angeles, Los Angeles, California 90095, United States; <https://orcid.org/0000-0002-7744-051X>*

**Ahamed Irshad** - *Department of Chemistry, University of Southern California, Los Angeles, California 90089, United States; <https://orcid.org/0000-0001-7107-9623>*

**Sangmin Kim** - *Department of Chemistry and Biochemistry, University of California, Los Angeles, Los Angeles, California 90095, United States; <https://orcid.org/0000-0002-7289-0693>*

**Mary A. Waddington** - *Department of Chemistry and Biochemistry, University of California, Los Angeles, Los Angeles, California 90095, United States*

**Charlene Z. Salamat** - *Department of Chemistry and Biochemistry, University of California, Los Angeles, Los Angeles, California 90095, United States; <https://orcid.org/0000-0001-5581-5029>*

**Milan Gembicky** - *Department of Chemistry and Biochemistry, University of California, San Diego, La Jolla, California 92093, United States; <https://orcid.org/0000-0002-3898-1612>*

**Arnold L. Rheingold** - *Department of Chemistry and Biochemistry, University of California, San Diego, La Jolla, California 92093, United States*

**Veronica Carta** - *Department of Chemistry and Biochemistry, University of California, Riverside, Riverside, California 92521, United States; <https://orcid.org/0000-0001-8089-8436>*

**Sarah Tolbert** - *Department of Chemistry and Biochemistry, University of California, Los Angeles, Los Angeles, California 90095, United States; Department of Materials Science and Engineering, University of California, Los Angeles, Los Angeles, California 90095, United States*

**Sri R. Narayan** - *Department of Chemistry, University of Southern California, Los Angeles, California 90089, United States*

### **Author Contributions**

The manuscript was written through contributions of all authors. All authors have given approval to the final version of the manuscript.

### **Notes**

The authors declare the following competing financial interest: UCLA Technology Development has filed a provisional patent application (PCT 63/350,759) based on the work presented; A. M. S. and his co-workers may receive royalty payments.

### **ACKNOWLEDGMENT**

This work was supported as part of the Center for Synthetic Control Across Length Scales for Advancing Rechargeables (SCALAR), an Energy Frontier Research Center funded by the U.S.

Department of Energy, Office of Science, Basic Energy Sciences under Award DE-SC0019381. A. M. S. thanks NIGMS (MIRA, R35GM124746), AFRL STTR (topic AF16-AT20) and the Dreyfus Foundation for the additional support. Y.A.N thanks the NSF for the Predoctoral (GRFP) Fellowship (DGE-2034835), The National GEM consortium for the GEM Fellowship, and UCLA for the Eugene V. Cota-Robles Fellowship. This material is based upon work partially supported by the National Science Foundation Graduate Research Fellowship Program under Grant No. (DGE-2034835). Any opinions, findings, and conclusions or recommendations expressed in this material are those of the author(s) and do not necessarily reflect the views of the National Science Foundation. The S10 program of the NIH Office of Research Infrastructure Programs, under grant S10OD028644, is acknowledged for the NEO600 in the NMR Facility. We thank Dr. Rafal Dziedzic, Dr. Alex Wixtrom, Ms. Emily Ganley, Ms. Ramya (Maya) Pathuri and Mr. Isaac Diaz for contributing to the preliminary synthetic routes towards some of the disclosed compounds. We are grateful to Dr. William Ewing (Boron Specialties) and Dr. Beth Bosley (Boron Specialties) for providing some of the  $B_{12}H_{12}$ -based precursors used in this project. The authors thank Mr. Billal Zayat for assistance with gold sputtering and Dr. Tyler Kerr for helpful discussions.

## REFERENCES

- (1) (a) Chen, E. Y.; Marks, T. J. Cocatalysts for metal-catalyzed olefin polymerization: activators, activation processes, and structure-activity relationships. *Chem. Rev.* **2000**, *100* (4), 1391-1434. DOI: 10.1021/cr980462j. (b) Fisher, S. P.; Tomich, A. W.; Lovera, S. O.; Kleinsasser, J. F.; Guo, J.; Asay, M. J.; Nelson, H. M.; Lavallo, V. Nonclassical Applications of closo-Carborane Anions: From Main Group Chemistry and Catalysis to Energy Storage. *Chem. Rev.* **2019**, *119* (14), 8262-8290. DOI: 10.1021/acs.chemrev.8b00551. (c) Hasegawa, A.; Ishihara, K.; Yamamoto, H. Trimethylsilyl pentafluorophenylbis(trifluoromethanesulfonyl)-methide as a super Lewis acid catalyst for the condensation of trimethylhydroquinone with isophytol. *Angew. Chem. Int. Ed.* **2003**, *42* (46), 5731-5733. DOI: 10.1002/anie.200352382. (d) Krossing, I.; Raabe, I. Noncoordinating anions - Fact or fiction? A survey of likely candidates. *Angew. Chem. Int. Ed.* **2004**, *43* (16), 2066-2090. DOI: 10.1002/anie.200300620. (e) Riddlestone, I. M.; Kraft, A.; Schaefer, J.; Krossing, I. Taming the Cationic Beast: Novel Developments in the Synthesis and Application of Weakly Coordinating Anions. *Angew. Chem. Int. Ed.* **2018**, *57* (43), 13982-14024. DOI: 10.1002/anie.201710782. (f) Strauss, S. H. The Search for Larger and More Weakly Coordinating Anions. *Chem. Rev.* **1993**, *93* (3), 927-942. DOI: DOI 10.1021/cr00019a005.
- (2) (a) Barbarich, T. J.; Handy, S. T.; Miller, S. M.; Anderson, O. P.; Grieco, P. A.; Strauss, S. H. LiAl(OC(Ph)(CF<sub>3</sub>)(2))(4): A hydrocarbon-soluble catalyst for carbon-carbon bond-forming reactions. *Organometallics* **1996**, *15* (18), 3776-3778. DOI: DOI 10.1021/om9604031. (b) Bernskoetter, W. H.; Schauer, C. K.; Goldberg, K. I.; Brookhart, M. Characterization of a Rhodium(I) sigma-Methane Complex in Solution. *Science* **2009**, *326* (5952), 553-556. DOI: 10.1126/science.1177485. (c) Brookhart, M.; Grant, B.; Volpe, A. F. [(3,5-(Cf<sub>3</sub>)<sub>2</sub>c<sub>6</sub>h<sub>3</sub>)<sub>4</sub>b]-[H(Oet<sub>2</sub>)<sub>2</sub>]<sup>+</sup> - a Convenient Reagent for Generation and Stabilization of Cationic, Highly

Electrophilic Organometallic Complexes. *Organometallics* **1992**, *11* (11), 3920-3922. DOI: DOI 10.1021/om00059a071. (d) Corey, J. Y. Generation of a Silicenium Ion in Solution. *J. Am. Chem. Soc.* **1975**, *97* (11), 3237-3238. DOI: DOI 10.1021/ja00844a063. (e) Ishihara, K.; Yamamoto, H. Arylboron compounds as acid catalysts in organic synthetic transformations. *Eur. J. Org. Chem.* **1999**, *1999* (3), 527-538. (f) Kobayashi, H.; Sonoda, T.; Iwamoto, H.; Yoshimura, M. Tetrakis [3,5-Di(F-Methyl)Phenyl]Borate as the 1st Efficient Negatively Charged Phase-Transfer Catalyst - Kinetic Evidences. *Chem. Lett.* **1981**, (5), 579-580. DOI: DOI 10.1246/cl.1981.579. (g) Krossing, I. The facile preparation of weakly coordinating anions: Structure and characterisation of silverpolyfluoroalkoxyaluminates  $\text{AgAl}(\text{ORF})(4)$ , calculation of the alkoxide ion affinity. *Chem. Eur. J.* **2001**, *7* (2), 490-502. DOI: Doi 10.1002/1521-3765(20010119)7:2<490::Aid-Chem490>3.0.Co;2-I. (h) Krossing, I.; Brands, H.; Feuerhake, R.; Koenig, S. New reagents to introduce weakly coordinating anions of type  $\text{Al}(\text{ORF})(4)(-)$ : synthesis, structure and characterization of Cs and trityl salts. *J. Fluorine. Chem.* **2001**, *112* (1), 83-90. DOI: Doi 10.1016/S0022-1139(01)00490-0. (i) Metz, M. V.; Sun, Y. M.; Stern, C. L.; Marks, T. J. Weakly coordinating Al-, Nb-, Ta-, Y-, and La-based perfluoroaryloxymetalate anions as cocatalyst components for single-site olefin polymerization. *Organometallics* **2002**, *21* (18), 3691-3702. DOI: 10.1021/om020087s. (j) Sun, Y. M.; Metz, M. V.; Stern, C. L.; Marks, T. J. Al-, Nb-, and Ta-based perfluoroaryloxide anions as cocatalysts for metallocene-mediated Ziegler-Natta olefin polymerization. *Organometallics* **2000**, *19* (9), 1625-1627. DOI: DOI 10.1021/om990946l.

(3) (a) Douvris, C.; Ozerov, O. V. Hydrodefluorination of perfluoroalkyl groups using silylium-carborane catalysts. *Science* **2008**, *321* (5893), 1188-1190. DOI: 10.1126/science.1159979. (b) Jelinek, T.; Plesek, J.; Hermanek, S.; Stibr, B. Chemistry of Compounds with the 1-Carba-Closo-Dodecaborane(12) Framework. *Collect. Czech. Chem. C.* **1986**, *51* (4), 819-829. DOI: DOI



10.1135/cccc19860819. (c) Liston, D. J.; Lee, Y. J.; Scheidt, W. R.; Reed, C. A. Observations on Silver Salt Metathesis Reactions with Very Weakly Coordinating Anions. *J. Am. Chem. Soc.* **1989**, *111* (17), 6643-6648. DOI: DOI 10.1021/ja00199a025. (d) Reed, C. A. Carboranes: A new class of weakly coordinating anions for strong electrophiles, oxidants, and superacids. *Accounts Chem. Res.* **1998**, *31* (3), 133-139. DOI: DOI 10.1021/ar970230r. (e) Shelly, K.; Finster, D. C.; Lee, Y. J.; Scheidt, W. R.; Reed, C. A. Eta-1-Benzene Coordination - the Synthesis and X-Ray Crystal-Structure of a Novel Silver Salt of the Weakly Coordinating Carborane Anion B11ch12-. *J. Am. Chem. Soc.* **1985**, *107* (21), 5955-5959. DOI: DOI 10.1021/ja00307a021. (f) Shelly, K.; Reed, C. A.; Lee, Y. J.; Scheidt, W. R. The Least Coordinating Anion. *J. Am. Chem. Soc.* **1986**, *108* (11), 3117-3118. DOI: DOI 10.1021/ja00271a058. (g) Xie, Z. W.; Manning, J.; Reed, R. W.; Mathur, R.; Boyd, P. D. W.; Benesi, A.; Reed, C. A. Approaching the silylium (R(3)Si(+)) ion: Trends with hexahalo (Cl, Br, I) carboranes as counterions. *J. Am. Chem. Soc.* **1996**, *118* (12), 2922-2928. DOI: DOI 10.1021/ja953211q. (h) Zakharova, I. A. Closoborate Anions as a Means of Synthesizing New Coordination-Compounds. *Coordin. Chem. Rev.* **1982**, *43*, 313-324. DOI: Doi 10.1016/S0010-8545(00)82102-5.

(4) (a) Douvris, C.; Michl, J. Update 1 of: Chemistry of the Carba-closo-dodecaborate(-) Anion, CB11H12-. *Chem. Rev.* **2013**, *113* (10), Pr179-Pr233. DOI: 10.1021/cr400059k. (b) Franken, A.; King, B. T.; Rudolph, J.; Rao, P.; Noll, B. C.; Michl, J. Preparation of [closo-CB<sub>11</sub>H<sub>12</sub>]<sup>(-)</sup> by dichlorocarbene insertion into [nido-B<sub>11</sub>H<sub>14</sub>]<sup>(-)</sup>. *Collect. Czech. Chem. C.* **2001**, *66* (8), 1238-1249. DOI: DOI 10.1135/cccc20011238. (c) Knoth, W. H. 1-B9h9ch- and B11h11ch-. *J. Am. Chem. Soc.* **1967**, *89* (5), 1274-&. DOI: DOI 10.1021/ja00981a048. (d) Plesek, J.; Jelinek, T.; Drdakova, E.; Hermanek, S.; Stibr, B. A Convenient Preparation of 1-CB<sub>11</sub>H<sub>12</sub><sup>-</sup> and Its C-Amino Derivatives. *Collect. Czech. Chem. C.* **1984**, *49* (7), 1559-1562. DOI: DOI 10.1135/cccc19841559.

(5) (a) Geis, V.; Guttsche, K.; Knapp, C.; Scherer, H.; Uzun, R. Synthesis and characterization of synthetically useful salts of the weakly-coordinating dianion  $[B_{12}Cl_{12}]^{(2-)}$ . *Dalton Trans.* **2009**, (15), 2687-2694. DOI: 10.1039/b821030f. (b) Knoth, W. H.; Muetterties, E. L.; Miller, H. C.; Chia, Y. T.; Sauer, J. C.; Balthis, J. H. Chemistry of Boranes .9. Halogenation of  $B_{10}H_{10}^{-2} + B_{12}H_{12}^{-2}$ . *Inorg. Chem.* **1964**, 3 (2), 159-&. DOI: DOI 10.1021/ic50012a002.

(6) (a) Avelar, A.; Tham, F. S.; Reed, C. A. Superacidity of Boron Acids H-2(B12X12) (X = Cl, Br). *Angew. Chem. Int. Ed.* **2009**, 48 (19), 3491-3493. DOI: 10.1002/anie.200900214. (b) Gu, W. X.; Ozerov, O. V. Exhaustive Chlorination of  $[B_{12}H_{12}]^{(2-)}$  without Chlorine Gas and the Use of  $[B_{12}Cl_{12}]^{(2-)}$  as a Supporting Anion in Catalytic Hydrodefluorination of Aliphatic C-F Bonds. *Inorg. Chem.* **2011**, 50 (7), 2726-2728. DOI: 10.1021/ic200024u. (c) Zhang, Y. B.; Liu, J. Y.; Duttwyler, S. Synthesis and Structural Characterization of Ammonio/Hydroxo Undecachloro-closo-Dodecaborates  $[B_{12}Cl_{11}NH_3]^{(-)}/[B_{12}Cl_{11}OH]^{(2-)}$  and Their Derivatives. *Eur. J. Inorg. Chem.* **2015**, (31), 5158-5162. DOI: 10.1002/ejic.201501009.

(7) Knoth, W. H.; Hertler, W. R.; Muetterties, E. L.; England, D. C.; Sauer, J. C. Chemistry of Boranes .19. Derivative Chemistry of  $B_{10}H_{10}^{-2} + B_{12}H_{12}^{-2}$ . *J. Am. Chem. Soc.* **1964**, 86 (19), 3973-&. DOI: DOI 10.1021/ja01073a015.

(8) Peymann, T.; Knobler, C. B.; Hawthorne, M. F. A study of the sequential acid-catalyzed hydroxylation of dodecahydro-closo-dodecaborate(2-). *Inorg. Chem.* **2000**, 39 (6), 1163-1170. DOI: DOI 10.1021/ic991105+.

(9) (a) Grisham, M. B.; Jefferson, M. M.; Melton, D. F.; Thomas, E. L. Chlorination of Endogenous Amines by Isolated Neutrophils - Ammonia-Dependent Bactericidal, Cyto-Toxic, and Cytolytic

Activities of the Chloramines. *J. Biol. Chem.* **1984**, *259* (16), 404-413. (b) Kelly, H. C.; Yasui, S. C.; Twissbrooks, A. B. Hypochlorite Chlorination of Tertiary Amine Boranes. *Inorg. Chem.* **1984**, *23* (15), 2220-2223. DOI: DOI 10.1021/ic00183a004.

(10) (a) Axtell, J. C.; Saleh, L. M. A.; Qian, E. A.; Wixtrom, A. I.; Spokoyny, A. M. Synthesis and Applications of Perfunctionalized Boron Clusters. *Inorg. Chem.* **2018**, *57* (5), 2333-2350. DOI: 10.1021/acs.inorgchem.7b02912. (b) Boere, R. T.; Derendorf, J.; Jenne, C.; Kacprzak, S.; Kessler, M.; Riebau, R.; Riedel, S.; Roemmele, T. L.; Ruhle, M.; Scherer, H.; et al. On the Oxidation of the Three-Dimensional Aromatics [B<sub>12</sub>X<sub>12</sub>](<sup>2-</sup>) (X=F, Cl, Br, I). *Chem. Eur. J.* **2014**, *20* (15), 4447-4459. DOI: 10.1002/chem.201304405. (c) Maderna, A.; Knobler, C. B.; Hawthorne, M. F. Twelfelfold functionalization of an icosahedral surface by total esterification of B-12(OH)<sub>12</sub> (<sup>2-</sup>): 12(12)-closures (vol 40, pg 1662, 2001). *Angew. Chem. Int. Ed.* **2001**, *40* (16), 2947-2947. DOI: Doi 10.1002/1521-3773(20010817)40:16<2947::Aid-Anie33332947>3.0.Co;2-X. (d) Miller, H. C.; Miller, N. E.; Muetterties, E. L. Synthesis of Polyhedral Boranes. *J. Am. Chem. Soc.* **1963**, *85* (23), 3885-&. DOI: DOI 10.1021/ja00906a033. (e) Pitochelli, A. R.; Hawthorne, M. F. The Isolation of the Icosahedral B<sub>12</sub>H<sub>12</sub>-2 Ion. *J. Am. Chem. Soc.* **1960**, *82* (12), 3228-3229. DOI: DOI 10.1021/ja01497a069. (f) Stauber, J. M.; Schwan, J.; Zhang, X. L.; Axtell, J. C.; Jung, D.; McNicholas, B. J.; Oyala, P. H.; Martinolich, A. J.; Winkler, J. R.; See, K. A.; et al. A Super-Oxidized Radical Cationic Icosahedral Boron Cluster. *J. Am. Chem. Soc.* **2020**, *142* (30), 12948-12953. DOI: 10.1021/jacs.0c06159.

(11) Tiritiris, I.; Schleid, T. The crystal structures of the dicesium dodecahalogeno-closedodecaborates CS<sub>2</sub>[B<sub>12</sub>X<sub>12</sub>] (X = Cl, Br, I) and their hydrates. *Z. Anorg. Allg. Chem.* **2004**, *630* (11), 1555-1563. DOI: 10.1002/zaac.200400167.

(12) (a) Hansen, B. R. S.; Paskevicius, M.; Jorgensen, M.; Jensen, T. R. Halogenated Sodium-closo-Dodecaboranes as Solid-State Ion Conductors. *Chem. Mater.* **2017**, *29* (8), 3423-3430. DOI: 10.1021/acs.chemmater.6b04797. (b) Jorgensen, M.; Jensen, S. R. H.; Humphries, T. D.; Rowles, M. R.; Sofianos, M. V.; Buckley, C. E.; Jensen, T. R.; Paskevicius, M. Hydroxylated closo-Dodecaborates  $M_2B_{12}(OH)_{12}$  ( $M = Li, Na, K, \text{ and } Cs$ ); Structural Analysis, Thermal Properties, and Solid-State Ionic Conductivity. *J. Phys. Chem. C.* **2020**, *124* (21), 11340-11349. DOI: 10.1021/acs.jpcc.0c02523. (c) Jorgensen, M.; Shea, P. T.; Tomich, A. W.; Varley, J. B.; Berx, M.; Lovera, S.; Cerny, R.; Zhou, W.; Udovic, T. J.; Lavallo, V.; et al. Understanding Superionic Conductivity in Lithium and Sodium Salts of Weakly Coordinating Closo-Hexahalocarborate Anions. *Chem. Mater.* **2020**, *32* (4), 1475-1487. DOI: 10.1021/acs.chemmater.9b04383.

(13) Ivanov, S. V.; Miller, S. M.; Anderson, O. P.; Solntsev, K. A.; Strauss, S. H. Synthesis and stability of reactive salts of dodecafluoro-closo-dodecaborate(2-). *J. Am. Chem. Soc.* **2003**, *125* (16), 4694-4695. DOI: 10.1021/ja0296374 From NLM PubMed-not-MEDLINE.

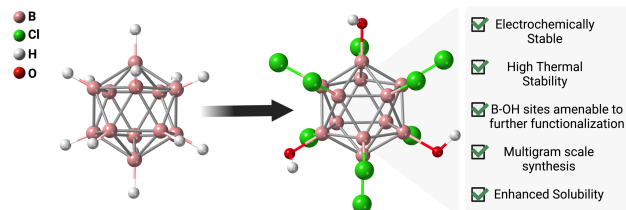
(14) Fang, Z.; Zhou, G. C.; Zheng, S. L.; He, G. L.; Li, J. L.; He, L.; Bei, D. Lithium chloride-catalyzed selective demethylation of aryl methyl ethers under microwave irradiation. *J. Mol. Catal. A Chem.* **2007**, *274* (1-2), 16-23. DOI: 10.1016/j.molcata.2007.04.013.

(15) (a) Aihara, J. Reduced HOMO-LUMO gap as an index of kinetic stability for polycyclic aromatic hydrocarbons. *J. Phys. Chem. A* **1999**, *103* (37), 7487-7495. DOI: DOI 10.1021/jp990092i. (b) Gao, Y.; Bulusu, S.; Zeng, X. C. Gold-caged metal clusters with large HOMO-LUMO gap and high electron affinity. *J. Am. Chem. Soc.* **2005**, *127* (45), 15680-15681. DOI: 10.1021/ja055407o. (c) Manolopoulos, D. E.; May, J. C.; Down, S. E. Theoretical-Studies of the Fullerenes - C<sub>34</sub> to C<sub>70</sub>. *Chem. Phys. Lett.* **1991**, *181* (2-3), 105-111. DOI: Doi

10.1016/0009-2614(91)90340-F. (d) McKee, M. L.; Wang, Z. X.; Schleyer, P. V. Ab initio study of the hypercloso boron hydrides B<sub>n</sub>H<sub>n</sub> and B<sub>n</sub>H<sub>n</sub><sup>-</sup>. Exceptional stability of neutral B<sub>13</sub>H<sub>13</sub>. *J. Am. Chem. Soc.* **2000**, *122* (19), 4781-4793. DOI: DOI 10.1021/ja994490a. (e) Parr, R. G.; Zhou, Z. X. Absolute Hardness - Unifying Concept for Identifying Shells and Subshells in Nuclei, Atoms, Molecules, and Metallic Clusters. *Accounts. Chem. Res.* **1993**, *26* (5), 256-258. DOI: DOI 10.1021/ar00029a005. (f) Pearson, R. G. Hard and Soft Acids and Bases. *J. Am. Chem. Soc.* **1963**, *85* (22), 3533-&. DOI: DOI 10.1021/ja00905a001. (g) Pearson, R. G. Hard and Soft Acids and Bases - the Evolution of a Chemical Concept. *Coordin. Chem. Rev.* **1990**, *100*, 403-425. DOI: Doi 10.1016/0010-8545(90)85016-L. (h) Zhan, C. G.; Nichols, J. A.; Dixon, D. A. Ionization potential, electron affinity, electronegativity, hardness, and electron excitation energy: Molecular properties from density functional theory orbital energies. *J. Phys. Chem. A* **2003**, *107* (20), 4184-4195. DOI: 10.1021/jp0225774. (i) Zhou, Z. X.; Parr, R. G.; Garst, J. F. Absolute Hardness as a Measure of Aromaticity. *Tetrahedron. Lett.* **1988**, *29* (38), 4843-4846. DOI: Doi 10.1016/S0040-4039(00)80623-1.

(16) Kweon, K. E.; Varley, J. B.; Shea, P.; Adelstein, N.; Mehta, P.; Heo, T. W.; Udovic, T. J.; Stavila, V.; Wood, B. C. Structural, Chemical, and Dynamical Frustration: Origins of Superionic Conductivity in closo-Borate Solid Electrolytes. *Chem. Mater.* **2017**, *29* (21), 9142-9153. DOI: 10.1021/acs.chemmater.7b02902.

## TOC



## SYNOPSIS

The heterofunctionalization process of the  $B_{12}H_{12}^{2-}$  cluster offers a promising approach to tailor the solubility, redox, and thermal stability of these boron-based weakly coordinating anions (WCAs). This work underscores the potential of B-OR site modification to expand the scope of existing WCAs and showcases the improved solubility characteristics of this new class of WCAs.